Engineering Electromagnetic Properties of Periodic Nanostructures Using Electrostatic Resonances

Gennady Shvets and Yaroslav Urzhumov
Department of Physics, The University of Texas at Austin, Austin, Texas 78712

Electromagnetic properties of periodic two-dimensional sub-wavelength structures consisting of closely-packed inclusions of materials with negative dielectric permittivity ϵ in a dielectric host with positive ϵ_h can be engineered using the concept of multiple electrostatic resonances. Fully electromagnetic solutions of Maxwell's equations reveal multiple wave propagation bands, with the wavelengths much longer than the nanostructure period. It is shown that some of these bands are described using the quasi-static theory of the effective dielectric permittivity ϵ_{qs}, and are independent of the nanostructure period. Those bands exhibit multiple cutoffs and resonances which are found to be related to each other through a duality condition. An additional propagation band characterized by a negative magnetic permeability develops when a magnetic moment is induced in a given nanoparticle by its neighbors. Imaging with sub-wavelength resolution in that band is demonstrated.

PACS numbers: 41.20.Cv, 42.70.Qs, 42.25.BS, 71.45.Gm

Electrostatic resonances of isolated nanoparticles have recently attracted substantial interest because of the intriguing possibility of obtaining very strong and localized electric fields. Applications of such fields include nanoscale biosensors [1, 2], nanolithography [3, 4], and nonlinear spectroscopy [5, 6]. Resonances occur when a metallic or dielectric particle with a negative frequency-dependent dielectric permeability $\epsilon(\omega) < 0$ is imbedded in a dielectric host (including vacuum) with a positive dielectric permeability $\epsilon_h > 0$. The wavelengths λ of the incident electromagnetic radiation that resonate with a small particle of a characteristic size $d \ll \lambda$ depend on the particle shape and the functional dependence of $\epsilon(\omega)$. By changing the shape [7] and internal composition [6] of nanoparticles resonances can be shifted to the wavelength optimized for a particular application. Close proximity of other small particles can also strongly affect the resonances. For example, disordered conglomerates of nanoparticles have recently been analyzed using the quasi-static theory [8] and shown [9] to exhibit multiple coherent "hot spots" that can be used for transporting electromagnetic energy. Surface-enhanced Raman scattering (SERS) from molecules inside multi-particle aggregates has also been shown to be greatly enhanced [10, 11, 12].

In this Letter we demonstrate how electrostatic resonances of *periodic* arrays of closely-spaced particles can be used for engineering propagation properties of electromagnetic radiation through such nanophotonic crystals. The emphasis of this work is on subwavelength photonic crystals (SPC) that have a periodicity d significantly smaller than the radiation wavelength in vacuum $\lambda \equiv 2\pi c/\omega$. By numerically solving Maxwell's equations, we identify two classes of waves supported by an SPC: (a) hybridized Dipole Modes (DM) that are characterized by a quasi-static period-independent dielectric permittivity $\epsilon_{qs}(\omega)$, and (b) hybridized Higher-order Multipole Modes (HMM) that depend on the crystal period d. Two types of DM's are identified: almost dispersionless (non-propagating) collective plasmons (CPL) satisfying the $\omega(\vec{k}) \equiv \omega_i^{(c)}$ dispersion relation (where $\omega_i^{(c)}$ are multiple zeros of ϵ_{qs}), and propagating collective photons (CPH) satisfying the $\vec{k}^2 c^2 = \omega^2 \epsilon_{qs}(\omega)$ dispersion relation. The mean-field dielectric permittivity ϵ_{qs} calculated from the quasi-static theory [8, 9] is found to be highly accurate in predicting wave propagation even for SPCs with the period as large as $\lambda/2\pi$. DM wave propagation bands are "sandwiched" between multiple resonance $\omega_i^{(r)}$ and the cutoff $\omega_i^{(c)}$ frequencies of the SPC. For two-dimensional SPC's with a high lattice symmetry (square and hexagonal) a duality condition expressing a simple one-to-one correspondence between the resonant and cutoff frequencies is derived.

The new HMM propagation bands are discovered inside the frequency intervals where $\epsilon_{qs} < 0$ and, by the mean-field description, propagation is prohibited. HMM bands should not be confused with the usual high order Brillouin zones of a photonic crystal because the latter do not satisfy the $d \ll \lambda$ condition. One HMM band defines the frequency range for which the sub-wavelength photonic crystal behaves as a double-negative metamaterial (DNM) that can be described by the negative effective permittivity $\epsilon_{eff} < 0$ and permeability $\mu_{eff} < 0$ [13]. Magnetic properties of the DNM are shown to result from the induced magnetic moment inside each nanoparticle by high-order multipole elecctrostatic resonances of its neighbors. It is shown that a thin slab of such DNM can be employed as sub-wavelength lens capable of resolving images of two slits separated by a distance $\ll \lambda$.

To start, consider a TM-polarized electromagnetic wave, with non-vanishing H_z, E_x, and E_y components, incident on an *isolated* dielectric rod (infinitely long in the $z-$direction) with $\epsilon(\omega) < 0$. The incident em wave is strongly scattered by the rod when its frequency ω coincides with that of the surface plasmon found by solving the nonlinear

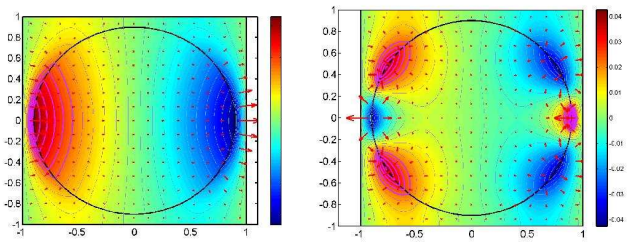

FIG. 1: Two strongest hybridized electrostatic dipole resonances of the 2-D square lattice of plasmonic rods contributing to ϵ_{qs}: $\omega_1^{(r)} = 0.38\omega_p$ (left); $\omega_2^{(r)} = 0.63\omega_p$ (right). Shown are the potential isocontours and the electric field arrows. Spatial dimensions are measured in $2c/\omega_p$ units. SPC parameters: $d = c/\omega_p$ and $R = 0.45d$.

eigenvalue equation for H_z:

$$-\vec{\nabla}\cdot\left(\epsilon^{-1}\vec{\nabla}H_z\right) = \frac{\omega^2}{c^2}H_z, \tag{1}$$

where $H_z \to 0$ far from the rod. The electric field of the surface wave is given by $\vec{E}(\vec{x}) = -i[c/\omega\epsilon(\vec{x})]\vec{e}_z \times \vec{\nabla}H_z$, where $\epsilon(\vec{x}) = \epsilon_h$ outside and $\epsilon(\vec{x}) = \epsilon(\omega)$ inside the rod. In what follows we assume that the rods are in vacuum, i. e. $\epsilon_h = 1$. Note that the lines $H_z = \text{const}$ are the electric field lines. For a sub-wavelength rod the rhs of Eq. (1) can be neglected. Moreover, $|\vec{E}| \gg |H|$, and the description using the electrostatic potential ϕ is appropriate: $\vec{E} = -\vec{\nabla}\phi$. Hence, two equations are simultaneously satisfied for a sub-wavelength rod:

$$-\vec{\nabla}\cdot\left(\epsilon^{-1}\vec{\nabla}H_z\right) = 0 \quad \text{and} \quad -\vec{\nabla}\cdot\left(\epsilon\vec{\nabla}\phi\right) = 0. \tag{2}$$

Equations (2) illustrate that in electrostatics there are two equivalent descriptions of the electric field: potential description and field line description. Note from Eqs. (2) that if a surface wave is supported by a rod of an arbitrary transverse shape for $\epsilon = \epsilon_1$, then a surface wave is also supported for $\epsilon = 1/\epsilon_1$ [7].

For a round cylinder of radius R the surface-wave multipole solutions of the second of Eqs. (2) are given by $\phi_{out}^{(m)} = (r/R)^{-m}\exp(im\theta)$ outside and $\phi_{in}^{(m)} = (r/R)^m\exp(im\theta)$ inside the cylinder, and $m \geq 1$. The continuity of $\epsilon\partial\phi/\partial r$ is satisfied for every $m \geq 1$ for $\omega^{(r)}$ such that $\epsilon(\omega^{(r)}) = -1$. This degeneracy of the multipole resonances is specific to the 2-D lattice of round cylinders. This property makes the square SPC of round cylinders particularly amenable to engineering its electromagnetic properties using electrostatic resonances: various multipoles of a given rod are strongly hybridized by the proximity of other rods. This gives rise to a rich and easily controllable set of hybridized electrostatic resonances whose frequencies depend on the areal fraction occupied by the cylinders. Earlier approximate calculations [14] of the three-dimensional lattice of metallic spheres failed to demonstrate the type of rich multi-resonant band structure found for 2-D structures and shown in Fig. 2 for two reasons: (a) there is no frequency degeneracy in three dimensions, and (b) the volume fraction occupied by metallic spheres is 3-D is smaller than in 2-D.

Note that there is no monopole ($m = 0$) *electrostatic* resonance (although there is an electromagnetic Mie resonance for rods with a very high positive ϵ [15]) for an isolated cylinder. Such a resonance would reveal that the corresponding solution for H_z has an associated azimuthal θ-independent current around the cylinder and, thus, a non-vanishing magnetic moment $M = (1/2c)\langle\vec{r}\times\vec{J}\rangle$, where the average is taken over the unit cell. However, as shown below, the octupole ($m = 4$) electrostatic resonances in a square lattice of closely-packed cylinders hybridize in a way of inducing a resonantly excited magnetic moment. This magnetic moment manifests itself as a negative effective permeability μ_{eff} of the structure, and an additional propagation band of DNW's in a narrow frequency range.

In the rest of the paper we concentrate on a specific SPC: a square lattice of round ($R = 0.45d$) *plasmonic* cylinders with $\epsilon(\omega) = 1 - \omega_p^2/\omega^2$ characteristic of collisions-free electron gas, lattice period $d = c/\omega_p$. Very similar results are expected for polaritonic rods with $\epsilon(\omega) = \epsilon_\infty(\omega^2 - \omega_{LO}^2)/(\omega^2 - \omega_{TO}^2)$, with $\epsilon < 0$ for $\omega_{TO} < \omega < \omega_{LO}$. To this SPC we apply the standard procedure [8, 9] for calculating the quasi-static dielectric permittivity $\epsilon_{qs}(\omega)$, and later compare the band structure described by $\epsilon_{qs}(\omega)$ to that obtained by solving the fully-electromagnetic Eq. 1.

The material-independent ϵ_{qs} is calculated [8, 9] as

$$\epsilon_{qs} = 1 - p\sum_{i=1}^{N}\frac{F_i}{s - s_i}, \tag{3}$$

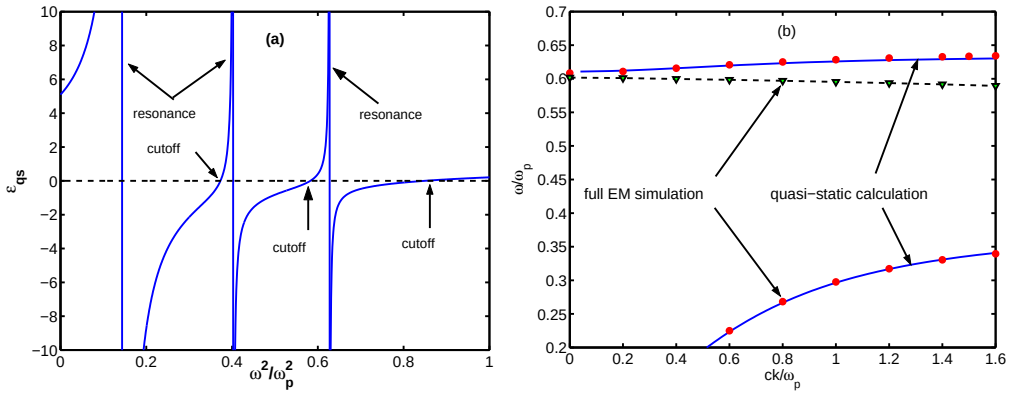

FIG. 2: (a) Frequency dependence of the quasi-static dielectric permittivity ϵ_{qs} from Eq. (3). Vertical lines: resonances, horizontal axis intercepts: cutoffs. (b) Collective photons (CPH) supported by the SPC: theoretical prediction of the quasi-static theory, $k = \sqrt{\epsilon_{qs}}\omega/c$ (solid lines) and numerical simulation of Eq. (1) (circles and diamond). Note the backward-wave mode ($\partial\omega/\partial k < 0$) marked by diamonds which is not described by the quasi-static theory. SPC parameters as in Fig. 1.

where, for the plasmonic rods in vacuum, $s(\omega) = [1-\epsilon(\omega)]^{-1} = \omega^2/\omega_p^2$, $s_i \equiv [1-\epsilon_i]^{-1}$ is the i'th out of $N > 1$ hybridized dipole resonances, F_i its oscillator strength calculated below, and $p = \pi R^2/d^2$. Electrostatic resonances s_i are found by solving the eigenvalue equation for the potential eigenfunctions ϕ_i inside a unit cell of the structure:

$$\vec{\nabla}\cdot\left[\theta(\vec{x})\vec{\nabla}\phi_i\right] = s_i\nabla^2\phi_i, \tag{4}$$

where ϕ_i satisfies the following homogeneous conditions at the unit boundaries $(x,y) = (\pm d/2, \pm d/2)$: (a) ϕ_i and its derivatives are periodic; (b) $\phi_i(x = \pm d/2) = 0$; (c) $\partial_y\phi_i(y = \pm d/2) = 0$. Equation (4) follows from Eq. (2). Physically, these eigenfunctions describe the electric potential distribution when a vanishing ac voltage (with frequency ω such that $\epsilon(\omega) = \epsilon_i$) is applied between $x = \pm d/2$ capacitor plates. The capacitance of such an imaginary capacitor, equal to the ratio of the charge to the voltage drop, is given by $C = \epsilon_{qs}d$, and becomes infinite according to Eq. (3). Another eigenfunction $\tilde{\phi}_i$ corresponding to the voltage drop between $y = \pm d/2$ plates is obtained by a 90−degree spatial rotation of ϕ_i.

Because the square lattice is invariant with respect to the transformations of the C_{4v} point group [16], all periodic solutions transform according to one of the irreducible representations (irreps) of C_{4v}: four singlets (commonly labeled as A_1, A_2, B_1, and B_2) and one doublet E. The electrostatic eigenfunctions ϕ_i and $\tilde{\phi}_i$ have the symmetry of E. Inside a given rod each ϕ_i can be expanded as the sum of multipoles: $\phi_i(r,\theta) = \sum_{l=0}^{\infty} A_i^{(2l+1)}(r/R)^{2l+1}\cos(2l+1)\theta$. A straightforward calculation following Ref. [9] yields the oscillator strength proportional to the dipole component of ϕ_i: $F_i = \left(A_i^1\right)^2 / \sum_{l=0}^{\infty}(2l+1)\left(A_i^{2l+1}\right)^2$. For our structure there are three significantly strong hybridized dipole (E−symmetric) resonances : $(s_1 = 0.1433, F_1 = 0.8909)$, $(s_2 = 0.4025, F_2 = 0.064)$, and $(s_3 = 0.6275, F_3 = 0.0366)$.

The plots of the two lowest resonances are shown in Fig. 1. The first resonance is primarily dipolar ($\propto\cos\phi$) while the second one has a significant sextupolar ($\propto\cos 3\phi$) component. Thus, the close proximity of the rods in the lattice results in a strong hybridization of the odd multipoles with the dipole. Moreover, the hybridized dipole resonances $\omega_1^{(r)} = 0.38\omega_p$, $\omega_2^{(r)} = 0.63\omega_p$, and $\omega_3^{(r)} = 0.79\omega_p$ occur at the frequencies *controllably* different (through the R/d ratio) from that of an isolated rod, $\omega^{(r)} = \omega_p/\sqrt{2}$.

The frequency dependence of the ϵ_{qs} for a plasmonic material is plotted in Fig. 2(a). The vertical lines in Fig. 2(left) are the plasmonic structure resonances which occur at $\omega_1^{(r)} = 0.38\omega_p$, $\omega_2^{(r)} = 0.63\omega_p$, and $\omega_3^{(r)} = 0.79\omega_p$. Quasi-static theory predicts no propagation in the region of $\epsilon_{qs} < 0$. Three frequencies $\omega_i^{(c)}$ for which $\epsilon_{qs}(\omega_i^{(c)}) = 0$ are called the cutoff frequencies. From Fig. 2(a), there are four propagation bands (where $\epsilon_{qs} > 0$) allowed by the quasi-static theory for $\omega < \omega_p$. The quasi-static theory predicts that this plasmonic SPC acts as an effective medium supporting two types of waves: four collective photons (CPHs) satisfying the $|\vec{k}|^2 = \epsilon_{qs}\omega^2/c^2$ dispersion relation (two of which are indicated by a solid line in Fig. 2(b)), and three non-propagating collective plasmons (CPLs) satisfying the $\omega(\vec{k}) = \omega_i^{(c)}$ dispersion relation (not shown). Numerical solutions of the fully electromagnetic Eq. (1) described below confirm these conclusions, yet reveal additional modes whose behavior *is not* described by the quasi-static ϵ_{qs}.

An important duality principle for the cutoff and resonance frequencies exists for square and hexagonal lattices (correspondingly invariant with respect to the C_{4v} and C_{6v} point group transformations): for each resonance frequency $\omega_j^{(r)}$ there exists a cutoff frequency $\omega_i^{(c)}$ for which $s\left(\omega_i^{(c)}\right) = 1$. This principle follows from an observation that, at

the cutoff, H_z satisfying the first Eq. (2) obeys the same boundary conditions as ϕ and $\tilde{\phi}$. Hence, from Eq. (2) follows that for each resonance frequency $\omega_j^{(r)}$ there exists a cutoff frequency $\omega_i^{(c)}$ for which $\epsilon(\omega_i^{(c)}) = 1/\epsilon(\omega_j^{(r)})$. Numerical calculation of the zeros of $\epsilon(s)$ from Eq. (3) indeed confirms the duality principle.

To verify that ϵ_{qs} is sufficient for accurate description of em wave propagation through the plasmonic SPC, the fully electromagnetic Eq. (1) was numerically solved as a nonlinear eigenvalue equation for ω^2/ω_p^2 for different wavenumbers $\vec{k} = \vec{e}_x k$, and the resulting dispersion relation $\omega(k)$ plotted in Fig. 2(b) for three propagation bands. Although $d = 1/\omega_p$ is not infinitesimally small compared to the radiation wavelength, it is apparent from Fig. 2 that the numerically calculated points (circles) accurately fall on the solid lines predicted for the CPH's by the scale-independent ϵ_{qs}. The essentially flat propagation band $\omega(k) \approx 0.61\omega_p$ not shown in Fig. 2(b) also agrees with the CPL dispersion relation obtained from ϵ_{qs}. Therefore, for several frequency bands, the plasmonic SPC indeed is an effective medium described by the scale-independent ϵ_{qs}.

Importantly, Fig. 2(b) reveals that there is another propagation band (diamonds) in the frequency range for which no propagation is expected due to $\epsilon_{qs} < 0$. Note that the mode's group velocity $v_g = \partial\omega/\partial k < 0$ opposes its phase velocity – an indication that we're dealing with a DNM. For $\vec{k} = 0$ this mode's H_z has the symmetry of the A_1 irrep of the symmetry group C_{4v}, and can be expanded inside a given plasmonic rod as $H_z(r,\theta) = \sum_{k=0}^{\infty} A^{(4k)} \left[I_{4k}(\omega\sqrt{-\epsilon}r/c)/I_{4k}(\omega\sqrt{-\epsilon}R/c)\right] \cos(4k\theta)$, where I_l is the modified Bessel function of order l. Because there is no dipole component in H_z, the A_1 mode does not contribute to the quasi-static permittivity ϵ_{qs}. For the SPC at hand, the largest term in the expansion is the octupole term $A^{(4)}$, and the next largest is the monopole term $A^{(0)}$ that is responsible for the magnetic moment induced in the photonic structure as explained earlier. Therefore, the mode is an HMM, with predominantly $m = 4$ component. Because of the finite magnetic moment, a single quantity ϵ_{qs} cannot describe the HMR resonances, and two frequency-dependent parameters are numerically evaluated: dielectric permittivity ϵ_{eff} and magnetic permeability μ_{eff}. The procedure for expressing these effective quantities for a periodic structure using the cell-averaged electric and magnetic fields has been described elsewhere [15, 17].

For two dimensions, and assuming that the elementary cell of the SPC is centered at the origin, we introduce several variables by averaging H_z and $\vec{E}$ over the sides or the area of the elementary cell of the photonic crystal: $\tilde{B}_z = d^{-2}\int dA H_z(x,y)$, $\tilde{H}_z = H_z(x = -d/2, y = -d/2)$, $\tilde{E}_y = d^{-1}\int_{-d/2}^{+d/2} dy\ E_y(x = -d/2, y)$, and $\tilde{D}_y = d^{-1}\int_{-d/2}^{d/2} dx E_y(x, y = -d/2)$. For $\vec{k} = k\vec{e}_x$ Maxwell's equations in the integral form become $kcg(kd)\tilde{E}_y = \omega\tilde{B}_z$ and $kcg(kd)\tilde{H}_z = \omega\vec{D}_y$, in complete correspondence with Maxwell's equations in the medium for which $\tilde{B}_z = \mu_{eff}\tilde{H}_z$ and $\tilde{D}_y = \epsilon_{eff}\tilde{E}_y$. Dimensionless factor $g(x) = i[1 - \exp(ix)]/x \to 1$ for $kd \ll 1$ is the slight modification accounting for non-vanishing lattice period.

The magnetic permeability μ_{eff} is affected because the mode carries the electric current which produces a finite magnetic moment. The magnetic nature of the A_1 mode is due to the non-vanishing coefficient of the monopole $A^{(0)}$ term in the multipole expansion. The monopole is responsible for the θ-independent component of the azimuthal electric field $E_\theta = -i[c/\omega\epsilon(r)]\partial_r H_z$. The corresponding electric current in the negative-ϵ rod given by $J_\theta = -A^{(0)}\omega/c(1 - 1/\epsilon)I_1(\omega r/c)/I_0(\omega r/c)$ produces a magnetic moment density $\vec{M} = (1/2c)\langle\vec{r} \times \vec{e}_\theta J_\theta\rangle$, where the average is taken over the unit cell, and can be shown to be $M = -(pA_0/4\pi)(1 - 1/\epsilon)I_2(\omega R/c)/I_0(\omega R/c)$.

The effective permittivity and permeability have been calculated for a range of wavenumbers $\vec{k} = k\vec{e}_x$ and the corresponding frequencies $\omega(k)$. For $kd \ll \pi$ it follows from the analyticity of $\omega(\vec{k})$ that the frequency depends only on $|\vec{k}|$ and not on its direction. For $k_0 = 0.6/d$ and $\omega_0 = 0.6\omega_p$ (or $n_{eff} = -1$) we numerically computed that $\mu_{eff} = -2.35$ and $\epsilon_{eff} = -0.427$. Therefore, at this frequency our SPC is a DNM. Note that the hybridized monopole/octupole resonance affects not only the magnetic permeability of the SPC, but also the dielectric permittivity: the mean-field calculation using Eq. (3) yields $\epsilon_{qs}(\omega_0) = -0.65$ that is significantly different from ϵ_{eff}.

DNM-based flat super-lenses capable of sub-wavelength imaging have been proposed [18]. The condition for super-lensing is that the DNM with the dielectric permittivity $\epsilon < 0$ is embedded in a host medium with $\epsilon_h = -\epsilon$. We have tested a six-period thick plasmonic SPC for the super-lensing effect by embedding it inside the hypothetic host with $\epsilon_h = 0.55$. This particular choice of $-\epsilon_{eff} < \epsilon_h < -\epsilon_{qs}$ was not optimized, and is one among the several that showed super-lensing. To verify the sub-wavelength resolution, we simulated the distribution of the magnetic field $|\vec{E}|$ behind a screen with narrow slits of width $\Delta_y = \lambda/5$ separated by a distance $2\Delta_y$. As depicted in Fig. 3, where only two slits are shown, a planar wave with frequency $\omega = 0.6\omega_p$ is incident on the screen from the left. A six-period long plasmonic SPC of width $D = 0.6\lambda$ is positioned between $0 < x < D$. The distribution of $|\vec{E}|$ in the $x - y$ plane is shown in Fig. 3(a). Also, in Fig. 3(b) $|\vec{E}|$ is plotted in two cross-sections: the object plane right behind the screen (at $x = -D/2 + \lambda/10$, solid line), and in the image plane (at $x = 3D/2 - \lambda/10$, dashed line). Object plane is slightly displaced from the screen to avoid $\vec{E}$-field spikes at the slit edges. The two sub-wavelength slits are clearly resolved. Increasing the incident frequency by just one percent (outside of the DNM band) results in the complete

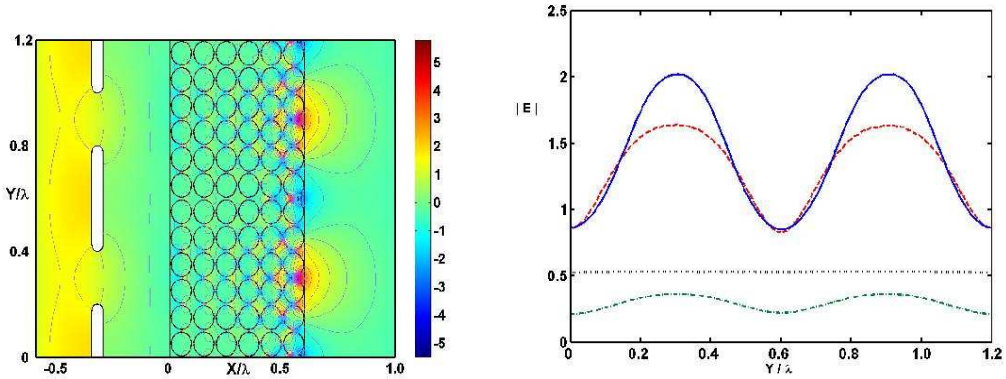

FIG. 3: (a) Magnetic field distribution behind an illuminated periodic slit array, with a six-period SPC, parameters as in Fig. 1. (b) $|\vec{E}|$ in the object plane (solid line); in the image plane for $\omega_0 = 0.6\omega_p$, without damping (dashed line) and with damping characteristic of silver (dot-dashed line); in the image plane for $\omega = 0.606\omega_p$ (dotted line).

loss of resolution in the image plane (dotted line).

While the DNM band for the plasmonic SPC is quite narrow, $[\omega(k=0) - \omega(k=\pi/d)]/\omega(k=0) = 0.055$, it is still broader than the collisional linewidth for some plasmonic materials. For example, for silver $\epsilon = \epsilon_b - \omega_p^2/\omega(\omega + i\gamma)$, where $\epsilon_b \approx 5$, $\omega_p = 9.1$ eV, and $\gamma = 0.02$ eV [19]. Fig. 3(b) (dash-dotted line) confirms that, although finite damping $\gamma/\omega_p = 0.002$ reduces the field amplitude in the image plane, it does not affect the image contrast. The band flatness in a plasmonic SPC translates into very sharp excitation resonances, and large enhancements of the incident field. For example, the very close proximity of two flat propagation bands in Fig. 3(b) (second DM and the A_1 HMM) can be exploited for maximizing the structure response at the incident and Raman-shifted re-emitted frequencies, which is essential for SERS.

This work is supported by the NSF's Nanoscale Exploratory Research Contract No. DMI-0304660.

[1] A. J. Hayes and R. P. V. Duyne, J. Chem. Phys. **124**, 10596 (2002).
[2] B. B. Akhremitchev, Y. Sun, L. Stebounova, and G. C. Walker, Langmuir **18**, 5325 (2002).
[3] M. M. Alkaisi, R. J. Blaikie, S. J. McNaub, R. Cheung, and D. R. S. Cumming, Appl. Phys. Lett. **75**, 3560 (1999).
[4] J. C. Hulteen, D. A. Treichel, M. T. Smith, M. L. Duval, T. R. Jensen, and R. P. van Duyne, J. Phys. Chem. B **103**, 3854 (1999).
[5] T. L. Haslett, L. Tay, and M. Moscovits, J. Chem. Phys. **113**, 1641 (2000).
[6] J. B. Jackson, S. L. Westcott, L. R. Hirsch, J. L. West, and N. J. Halas, Appl. Phys. Lett. **82**, 257 (2003).
[7] D. R. Fredkin and I. D. Mayergoyz, Phys. Rev. Lett. **91**, 253902 (2003).
[8] D. J. Bergman and D. Stroud, Solid State Physics **46**, 147 (1992).
[9] M. I. Stockman, S. V. Faleev, and D. J. Bergman, Phys. Rev. Lett. **87**, 167401 (2001).
[10] A. M. Michaels, J. Jiang, and L. Brus, J. Phys. Chem. **104**, 11965 (2000).
[11] V. A. Markel, V. M. Shalaev, P. Zhang, W. Huynh, L. Tay, T. L. Haslett, and M. Moscovits, Phy. Rev. B **59**, 10903 (1999).
[12] D. A. Genov, A. K. Sarychev, V. M. Shalaev, and A. Wei, Nano Letters **4**, 153 (2004).
[13] D. R. Smith, D. C. Vier, N. Kroll, and S. Schultz, Appl. Phys. Lett. **77**, 2246 (2000).
[14] W. Lamb, D. M. Wood, and N. W. Ashcroft, Phys. Rev. B **21**, 2248 (1980).
[15] S. O'Brien and J. B. Pendry, Journ. Phys. Cond. Matt. **14**, 4035 (2002).
[16] G. Y. Lyubarskii, *Application of Group Theory in Physics* (Pergamon Press, New York, 1960).
[17] J. B. Pendry, A. J. Holden, D. J. Robbins, and W. J. Stewart, IEEE Trans. Microwave Theory Tech. **47**, 2075 (1999).
[18] J. B. Pendry, Phys. Rev. Lett. **85**, 3966 (2000).
[19] P. B. Johnson and R. W. Christy, Phys. Rev. B **6**, 4370 (1972).